Autonomous Robots 17, 23–39, 2004

Distributed Cooperative Outdoor Multirobot Localization and Mapping

RAJ MADHAVAN
Intelligent Systems Division, National Institute of Standards and Technology, Gaithersburg, MD 20899-8230, USA
raj.madhavan@ieee.org

KINGSLEY FREGENE
Honeywell Laboratories, 3660 Technology Drive, Minneapolis, MN 55418, USA
kocfrege@ieee.org

LYNNE E. PARKER
Department of Computer Science, University of Tennessee, Knoxville, TN 37996-3450, USA
parker@cs.utk.edu

Abstract. The subject of this article is a scheme for distributed outdoor localization of a team of robots and the use of the robot team for outdoor terrain mapping. Localization is accomplished via **E**xtended **K**alman **F**iltering (EKF). In the distributed EKF-based scheme for localization, heterogeneity of the available sensors is exploited in the absence or degradation of absolute sensors aboard the team members. The terrain mapping technique then utilizes localization information to facilitate the fusion of vision-based range information of environmental features with changes in elevation profile across the terrain. The result is a terrain matrix from which a metric map is then generated. The proposed algorithms are implemented using field data obtained from a team of robots traversing an uneven outdoor terrain.

Keywords: multirobot localization, terrain mapping, heterogeneous sensing, extended Kalman filter

1. Introduction

The development of unmanned mobile robotic systems that operate in complex and highly dynamic environments has received tremendous interest from roboticists in recent years. In the last decade or so, the notion of having a team of robots cooperate to achieve a goal has gained due attention since such a scheme offers several advantages for various application domains (Feddama et al., 2000; Gage and Pletta, 1987). However, the realization of a multirobot system is not without some difficulties compared to single robot systems (Parker, 2000; Cao et al., 1997).

Two types of architectures, *centralized* and *decentralized*, can be employed to achieve cooperation in a robot team. In a centralized architecture, all planning, execution control and monitoring tasks are performed by a single control unit. It is considerably difficult to have a *fully* centralized scheme for the control of multiple robots as the computational overhead increases exponentially with the number of robots in the team. When there is no central processing facility and all the decisional issues for a team member are tackled within the robot itself, some of the disadvantages associated with centralized architectures (e.g., high computational burden, single point of failure, complex control logic design, etc.) can be overcome. This motivation has manifest itself into decentralized (and distributed) architectures that provide more robust and modular capabilities (Parker, 2000).

In this article, we consider the localization of a team of robots in an unknown, unstructured outdoor

environment and the mapping of this terrain by the robot team (Madhavan et al., 2002; Fregene et al., 2002). Localization, the process of determining the position and orientation (pose) of a robot within the operating environment, is critical for subsequent high level navigation tasks like path-planning in realistic outdoor environments and terrain mapping. Such maps should provide information about the location of objects/features in the environment and what the elevation gradient (or variation) is across the area. This information facilitates the planning of paths that are optimal in some sense (e.g., the distance between origin and goal locations, the amount of energy expended, etc.).

Each member of the *heterogeneous*[1] robot team considered in this article possesses absolute positioning capability by means of differential GPS (DGPS). Unfortunately, multipathing errors make it extremely difficult to localize based solely on DGPS. Thus, it becomes necessary to develop a framework within which observations from dead-reckoning and absolute sensors can be *fused* to continually deliver reliable and consistent pose estimates. Additionally, in order to minimize the computational bottlenecks associated with centralized architectures, we seek to decentralize the multirobot localization and mapping process across the members of the group.

To achieve the above requirements, a distributed **E**xtended **K**alman **F**ilter-based algorithm for the localization of a team of robots operating in an outdoor terrain is developed in this article. The associated terrain mapping algorithm is based on merging multiple local maps obtained by each member of the vehicle team during specific motion segments into a globally consistent metric map. The local maps combine the elevation gradient and vision-based depth (i.e., ranges) to environmental features using the pose estimates provided by the EKF. Each local map is obtained while the robots systematically traverse the terrain by navigating to and around an object of interest (OOI). This bears some resemblance to the notion of *frontiers* used in Yamauchi (1998) to the extent that the robots explore different regions delineated by OOI's. Our approach differs in the autonomous manner in which the regions are specified and in the fact that elevation information is directly utilized. In the proposed scheme, a coordinate frame centered at the location of the DGPS base station is fixed to the environment of interest. Because this is a global reference frame (from the point of view of each robot) merging locally generated maps becomes easier.

In the first part of the article, we show that distributed localization of robot team members can be realized in a straightforward manner by enabling each robot to maintain its pose using an EKF that is *local* to that particular robot. We also consider the case when all of the robots may not possess absolute positioning capabilities either due to the absence of requisite sensors or due to the degradation of available sensors. We show in such cases how multirobot cooperative localization can be achieved by exploiting heterogeneous sensors aboard the team members. The resulting pose estimates are then utilized in the second part of this article to develop the terrain mapping scheme.

This article is organized as follows: Section 2 briefly reviews previous cooperative localization and mapping schemes reported in the literature. Section 3 describes the distributed localization scheme. Section 4 develops heterogeneous cooperative localization approaches. The terrain mapping procedure is detailed in Section 5 followed by experimental results in Section 6. Section 7 provides the conclusions and indicates avenues by which the work described in this article can be extended.

2. Related Work

Several *robot-based* cooperative navigation approaches have been presented in the literature (Premvuti and Wang, 1996; Bison and Trainito, 1996; Kurazume et al., 1996). The underlying idea in such schemes is that one member of the team uses another member of the team for realizing cooperative navigation. The main limitations of such approaches are that: (1) only one robot is allowed to move prior to the movement of the other members of the team, (2) the robots have to move in such a way that they can "see" each other, which necessitates visual (sensorial) contact to be maintained at *all* times, and (3) the coordination abilities of the team as a whole suffer as the tasks are carried out in groups.

Collaborative multirobot localization, within an estimation-theoretic framework, have been considered by many authors. Fox et al. perform collaborative localization of two indoor robots equipped with a model of the environment using a sample-based version of the Monte Carlo Localization (MCL) algorithm (Fox et al., 1999). The main strength of MCL is its ability to perform *global* localization. It is not clear how well it will perform when extended to unstructured

domains and slippery terrain. Sanderson formulates the cooperative navigation problem in a Kalman filter (KF) framework (Sanderson, 1996). In the proposed Cooperative Navigation System (CNS), inter-robot positions are treated as observations and the KF estimates the position of all robots simultaneously. The CNS algorithm has been tested on two Yamabico robots in an indoor environment equipped with ultrasonic sensors by which one robot can sense the position of the other robot. It is not clear whether a centralized or a decentralized methodology is adopted for exchange of sensing information and subsequent state estimate updates.

Roumeliotis et al. (2002) present a KF-based distributed localization approach for cooperative localization. A centralized KF performs data fusion by using observations from a group of mobile robots. Both proprioceptive (relative) and exteroceptive (absolute) sensors are employed. The standard KF prediction equations are decentralized and distributed among the robots in the team. It is argued that the multirobot localization problem renders the state propagation equations of the centralized system to be decoupled with state coupling occurring only when relative pose observations become available. Whenever two robots meet, the relative pose information obtained from a camera tracking system is used to centrally update the pose estimates of the robot team members. The results are verified on an indoor robot team.

On the cooperative mapping front, Burgard et al. detail an explicit coordination mechanism that assigns appropriate target points to indoor robots in a team such that they effectively explore different regions (Burgard, et al., 2000) using an occupancy grid map that is built based on the data sensed by individual robots. Similar to Roumeliotis et al. (2002), the relative position between robots is assumed to be known. A dead-reckoning-free robust positioning system for global mapping using multiple mobile robots is described by Dudek et al. (1993) by having the robots define a local coordinate system without reference to environmental features. In this *robot-based* representation, sensing errors remain localized to the individual robot. Inter-robot positions are determined by metric information but the resulting global map describes the neighbor relations between the robots in the form of a graph. Rekleitis et al. (1998) report a graph-based exploration strategy for map construction in which two Real World Interface (RWI) B12 robots act in concert to reduce odometry errors. Each robot is equipped with a *robot tracker* sensor which tracks a geometric target installed on the other robot visually. In this scheme, the distance from one robot to the other is inferred from the height of the stripe pattern in the image. The limitation of the approaches in Dudek et al. (1993) and Rekleitis et al. (1998) lies in the fact that the robots cannot be distributed over the operating environment as they are required to remain close to each other to maintain visibility.

Cooperative localization and occupancy-grid mapping of two homogeneous indoor robots each equipped with a stereo-vision head is described by Jennings et al. (1999) and Little et al. (1998). Although grid-based maps have the advantage of allowing explicit modeling of free-space and ease of fusing data from different sensors (Grabowski, 2000; Yamauchi, 1998), they are often impractical for large unstructured environments due to the fixed grid-size and the accompanying computational burden. Additionally, false alarms and data association ambiguities are difficult to incorporate. Howard and Kitchen (1999) describe a cooperative localization and mapping (CLAM) scheme in which two robots coordinate to reduce odometric uncertainty during unknown indoor environment exploration. Each robot is equipped with a color camera so that they 'recognize' each other using colored tags around their base. A disadvantage of this approach is that at any given instant, only one robot of the team is allowed to move. In this way, the stationary robot estimates its own position with increased certainty than possible by odometry alone. This tends to limit both the speed and the accuracy of the maps that are constructed. Another disadvantage is that both the proposed cooperative localization and mapping approaches are centralized as opposed to the distributed approach we have adopted.

It is important to note that the focus of the present work is primarily on CLAM and not (the related area of) SLAM. This is why the growing literature in SLAM is not reviewed in great detail here. The interested reader is therefore referred to works like (Di Marco et al., 2003; Jung et al., 2002) and references therein for more information.

From the brief review above, it is evident that current cooperative robotic navigation research primarily concentrates on indoor environments. In *outdoor* environments, errors introduced due to distance traveled can be significant and unpredictable. This is a direct consequence of the undulatory nature of the terrain of travel and the uncertainties introduced into sensor data. The robots may also tip over or be inclined in such a way that sensors used for cooperative localization become ineffective. These challenges make it

comparatively difficult to realize successful navigation and mapping in unstructured outdoor environments.

Motivated by these factors, this article develops terrain-aided localization and mapping algorithms that possess the following strengths:

- It can cope with outages of absolute positioning systems either due to the absence of requisite sensors or due to the degradation of available sensors by exploiting heterogeneous sensors aboard the team members (e.g., ability to cope with DGPS outages).
- No absolute positioning system capable of providing relative pose information is assumed to be available. Even though we utilized DGPS, it provides accurate absolute position information only when sufficient number of satellites are in view at any given time.
- It can operate in unstructured and previously unmapped environments with no modifications to the operating environment or to the robots of the team.
- There is no restriction on how many robots can move at any instant.
- The sensors required are not unduly sophisticated thus making the schemes economically viable.

3. Distributed EKF Localization

The EKF (Maybeck, 1979) employed for the localization of the robots requires a kinematic (process) model and a sensor (observation) model. The experimental setup, the process and observation models, the ensuing estimation cycle and the corresponding experimental results are presented in the following paragraphs.

3.1. Experimental Setup and Sensor Calibration

The experimental platform is a team of **A**ll **T**er**R**ain **V**ehicles-Mini wheeled mobile robots with 4-wheel differential-drive skid-steering. The experimental setup consists of a wireless LAN (WLAN), Local Area DGPS (LADGPS), a software platform (*mobility* from RWI) and codes developed in-house under Linux. The WLAN is set up outdoors between an Operator Console Unit (OCU) and the robots. The OCU consists of a rugged laptop equipped with a BreezeCOM access point and antennas. Each robot has a station adapter and an antenna. The LADGPS is formed by the base station/antenna hardware connected to the OCU and remote stations/antennas directly mounted on each robot. Each robot's station receives differential corrections from the base station (sub-meter LADGPS accuracy was observed when 11 GPS satellites were acquired). The distributed CORBA-based interface offered by *mobility* ensures that querying the sensor slots of particular robots is done in a transparent decentralized manner by simply appending the robot's ID to all such queries.

The sensor suite for localization and mapping (shown in Fig. 1) is comprised of encoders that measure the wheel speeds and heading, DGPS, magnetic compass, a pan-tilt-zoom (PTZ) capable camera for visual perception, inclinometers, and a scanning laser rangefinder (not shown in this particular robot). The PTZ camera has a focal length in the range 5.4–64.8 mm (i.e., a variable zoom system). Its pixel resolution is 120×160 with a 37° field of view (FOV). Table 1 summarizes the sensor suite and its characteristics.

Since the experiments are carried out in an outdoor environment with the robots executing general motion

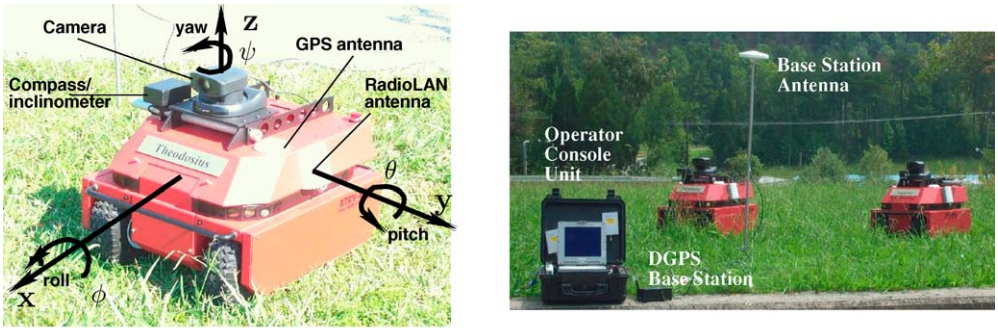

(a) (b)

Figure 1. The ATRV-Mini sensor suite and experimental setup. The sensor suite shown in (a) consists of encoders, DGPS, a compass and a PTZ camera (also see Table 1). The experimental setup depicted in (b) consists of an operator console unit, a DGPS base station and a base station antenna. See text for further details.

Table 1. Sensor suite description.

Sensor	Description	Freq. (Hz)
`Odometry`	Provides wheel speed and rate of change of heading (relative)	≈50
`DGPS`	Provides (x, y) position of robots (absolute)	≈1
`Vision`	Provides images using a pan-tilt-zoom (PTZ) capable camera (absolute)	≈10
`Compass`	Provides heading with respect to true north (absolute)	≈1
`Inclinometers`	Provides pitch and roll angles to true north (absolute)	≈1
`Laser rangefinder`	Provides range and bearing to targets (absolute)	≈10

(translation and rotation on all axes), sensor calibration is important to ensure accuracy of readings. For the encoder readings, external sensors (DGPS and magnetic compass) are used to obtain calibration factors corresponding to the various axes. The correction factor for magnetic compass is obtained by looking up geodesic charts to determine the angle of magnetic variation corresponding to the longitude/latitude of the experiment's location.

3.2. ATRV-Mini Kinematic Model

For the ATRV-Mini, it is observed that the two wheel pairs may be rotated at different speeds. If both pairs are driven forward with the same speed, then the robot moves forward, but if they are driven in opposite directions, the robot will turn in place. Wheel pairs on the same side may also be rotated at different speeds thereby enabling the robot to make gradual turns as it traverses. This flexibility allows compact maneuvers to be effected, such as turning in place (i.e., executing a zero-radius turn). Skid-steering is difficult to model (Economou, 1999) as a skid-steering robot slips when it turns. It is our conclusion from the field trials that a no-slip kinematic model using encoder-based odometry in combination with external corrections from an absolute sensor suffices for localization.

The nominal (noise-free) discrete process model equations at time-instant k can be written as:

$$\begin{bmatrix} x_{v_k} \\ y_{v_k} \\ \phi_{v_k} \end{bmatrix} = \begin{bmatrix} x_{v_{k-1}} \\ y_{v_{k-1}} \\ \phi_{v_{k-1}} \end{bmatrix} + \Delta T \begin{bmatrix} V_k \cos \phi_{v_{k-1}} \\ V_k \sin \phi_{v_{k-1}} \\ \omega_k \end{bmatrix} \quad (1)$$

where ΔT is the synchronous sampling interval between states at discrete-time instants $(k-1)$ and k. The state vector given by $\mathbf{x}_k$: $(x_{v_k} y_{v_k} \phi_{v_k})$ denotes the (x, y) coordinates and heading of the robot's center of mass, respectively. The control signals applied to the vehicle are $\mathbf{u}_k = [V_k, \omega_k]$ where V_k is the linear velocity and ω_k is the heading rate of the robot at time-instant k. The errors due to the control signals V and ω are modeled as simple additive noise sources, δV and $\delta\omega$, about their respective means $\bar{V}$ and $\bar{\omega}$ as $V_k = \bar{V}_k + \delta V_k$ and $\omega_k = \bar{\omega}_k + \delta\omega_k$. The error source vector is defined as: $\delta\mathbf{w}_k = [\delta V_k, \delta\omega_k]^T$ and is a direct effect of the associated modeling errors and uncertainty in control. The source errors δV and $\delta\omega$ are assumed to be zero-mean, uncorrelated Gaussian sequences with constant variances σ_V^2 and σ_ω^2, respectively. The variances were determined experimentally to reflect true noise variances.

3.3. Observation Models

The observation model for DGPS and compass are given by:

$$\mathbf{z}_k^{\mathrm{g}} = \mathbf{H}_k^{\mathrm{g}} \mathbf{x}_k + v_k^{\mathrm{g}}; \quad \mathbf{H}_k^{\mathrm{g}} = \begin{bmatrix} 1 & 0 & 0 \\ 0 & 1 & 0 \end{bmatrix};$$
$$z_k^{\mathrm{c}} = \mathbf{H}_k^{\mathrm{c}} \mathbf{x}_k + v_k^{\mathrm{c}}; \quad \mathbf{H}_k^{\mathrm{c}} = [\,0 \quad 0 \quad 1\,];$$

where v_k^{g} and v_k^{c}, respectively, refer to the uncertainty present in DGPS and compass observations, and are modeled as zero-mean uncorrelated Gaussian sequences with constant variances, $\begin{bmatrix} \sigma_{x_g}^2 \\ \sigma_{y_g}^2 \end{bmatrix}$ and $\sigma_{\phi_c}^2$, respectively. The variances for the DGPS reported positions are set inversely proportional to the number of satellites in view (this design choice is motivated by what was observed experimentally).

3.4. Estimation Cycle

The predict-observe-validate-update estimation cycle of the EKF (Maybeck, 1979) for the localization of every robot team member proceeds as below:

- *Prediction*: The state prediction takes place according to Eq. (1) as follows:

$$\begin{bmatrix} x_{v_{(k|k-1)}} \\ y_{v_{(k|k-1)}} \\ \phi_{v_{(k|k-1)}} \end{bmatrix} = \underbrace{\begin{bmatrix} x_{v_{(k-1|k-1)}} \\ y_{v_{(k-1|k-1)}} \\ \phi_{v_{(k-1|k-1)}} \end{bmatrix} + \Delta T \begin{bmatrix} V_k \cos\phi_{v_{(k-1|k-1)}} \\ V_k \sin\phi_{v_{(k-1|k-1)}} \\ \omega_k \end{bmatrix}}_{\mathbf{f}_{\mathbf{x}_{v_k}}} \quad (2)$$

  The prediction covariance can now be computed using:

$$\mathbf{P}_{(k|k-1)} = \nabla\mathbf{f}_{\mathbf{x}_{v_k}} \mathbf{P}_{(k-1|k-1)} \nabla\mathbf{f}_{\mathbf{x}_{v_k}}^T + \nabla\mathbf{f}_{\mathbf{w}_k} \mathbf{Q}_k \nabla\mathbf{f}_{\mathbf{w}_k}^T$$

  where $\nabla\mathbf{f}_{\mathbf{x}_{v_k}}$ represents the Jacobian with respect to the states, $\nabla\mathbf{f}_{\mathbf{w}_k}$ is the Jacobian with respect to the error sources and $\mathbf{Q}_k$ is the noise strength matrix given by:

$$\nabla\mathbf{f}_{\mathbf{x}_{v_k}} = \begin{bmatrix} 1 & 0 & -\Delta T V_k \sin\phi_{v_{(k-1|k-1)}} \\ 0 & 1 & \Delta T V_k \cos\phi_{v_{(k-1|k-1)}} \\ 0 & 0 & 1 \end{bmatrix}$$

$$\nabla\mathbf{f}_{\mathbf{w}_k} = \Delta T \begin{bmatrix} \cos\phi_{v_{(k-1|k-1)}} & 0 \\ \sin\phi_{v_{(k-1|k-1)}} & 0 \\ 0 & 1 \end{bmatrix}$$

$$\mathbf{Q}_k = \begin{bmatrix} \sigma_{V_k}^2 & 0 \\ 0 & \sigma_{\omega_k}^2 \end{bmatrix}$$

- *Observation validation*: Once the predicted states and their covariances are available, the DGPS/compass observations that arrive are accepted only if the observation falls inside the normalized residual validation gate, $\nu_k^T \mathbf{S}_k^{-1} \nu_k \leq \epsilon_\gamma$, where ν_k is the residual defined as the difference between the actual and predicted positions. The value of ϵ_γ can be chosen from the fact that the normalized residual sequence is a χ^2 random variable with m degrees of freedom (m being the dimension of the observation) (Maybeck, 1979). The residual covariance is given by: $\mathbf{S}_k = \mathbf{H}_k \mathbf{P}_{(k|k-1)} \mathbf{H}_k^T + \mathbf{R}_k$.
- *Update*: Once a validated observation is available, the state estimate and covariance updates are performed using the EKF update equations (Maybeck, 1979):

$$\mathbf{x}_{(k|k)} = \mathbf{x}_{(k|k-1)} + \mathbf{W}_k \nu_k$$
$$\mathbf{P}_{(k|k)} = \mathbf{P}_{(k|k-1)} - \mathbf{W}_k \mathbf{S}_k \mathbf{W}_k^T$$

  where the Kalman gain matrix is given by

$$\mathbf{W}_k = \mathbf{P}_{(k|k-1)} \mathbf{H}_k^T \mathbf{S}_k^{-1}$$

3.5. Experimental Results for Localization

Figure 2 shows the estimated path, orientation of the robot, pose standard deviations of the estimated pose and the 95% confidence (2σ) bounds for the DGPS residual, respectively, for one of the robots of the team. The EKF-based localization algorithm continually corrects the diverging dead-reckoning estimates based on external sensing information provided by DGPS and compass corrections as reflected by the periodic rise and fall of the pose standard deviations in Fig. 2(c). The decrease in the standard deviations is due to the corrections offered by the DGPS/compass and the increase is due to the vehicle being localized based on prediction (dead-reckoning) alone. When the DGPS/compass do not provide aiding information towards the localization of the vehicle, the standard deviation is at a maximum. Due to the observation validation procedure, the residuals in Fig. 2(d) are clearly bounded and are indicative of consistent estimates. As the EKF "fuses" the encoder measurements along with the DGPS and compass readings to arrive at estimates, the EKF pose estimate is always superior than that provided by DGPS alone. Consequently, we are guaranteed a better position fix even when DGPS is subject to multipathing errors. Moreover, in our current setup DGPS does not provide orientation information.

4. Exploiting Heterogeneity for Cooperative Localization

When some robots of the team do not have absolute positioning capabilities or when the quality of the observations from the absolute positioning sensors deteriorate, another robot in the team (with better positioning capability) can assist in the localization of the robots whose sensors have deteriorated or failed. In such cases, if *relative pose* information is obtained, the EKF-based localization algorithm can be cast in

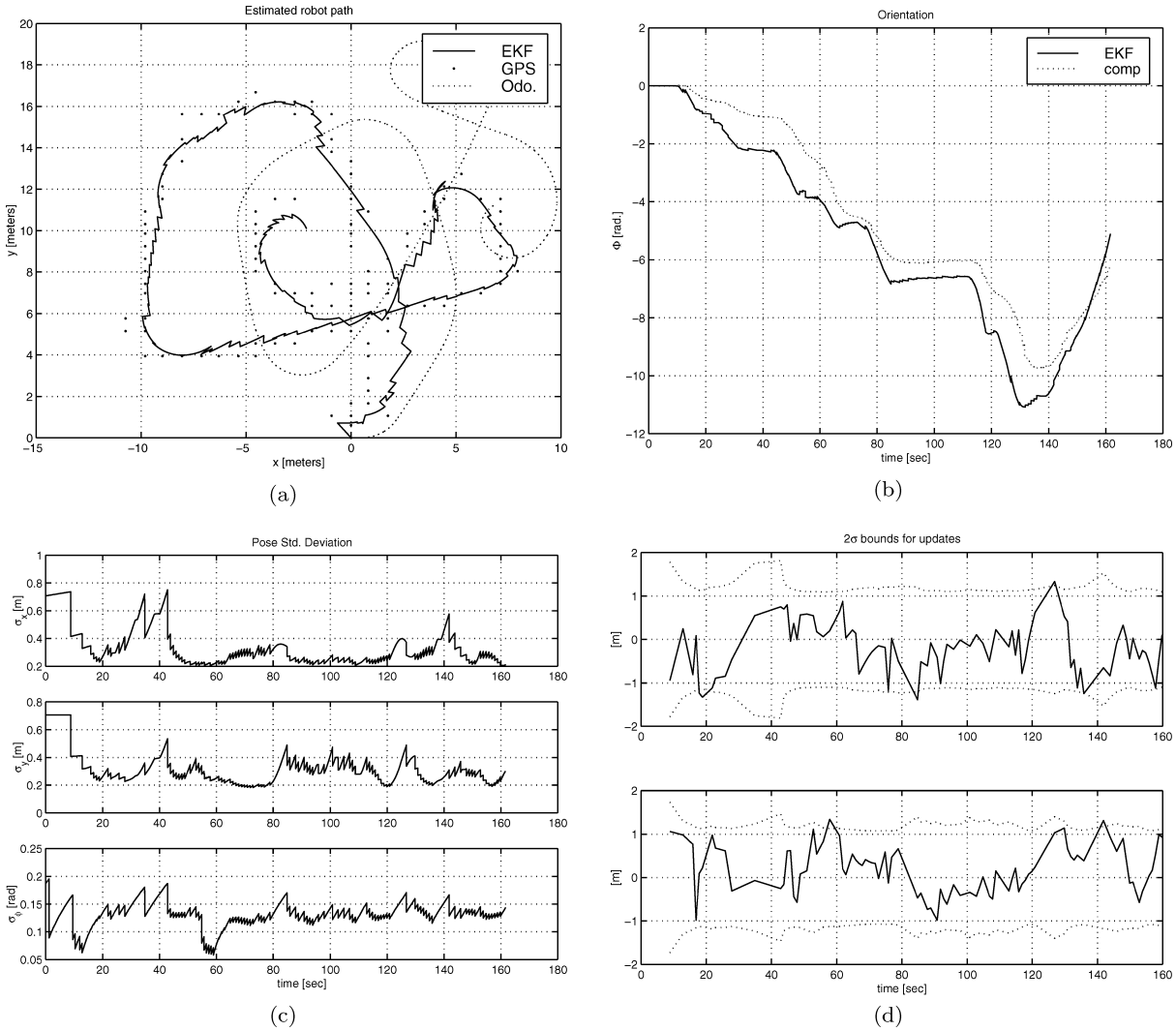

Figure 2. EKF estimated robot path is shown in (a) and orientation in (b). In (a), the robot starts at (0,0) and the dots represent the DGPS observations. The odometric path is plotted in (a) and the compass readings are plotted in (b) for comparison. The standard deviation of the pose is shown in (c) and the residual with the 95% (2σ) confidence bounds in (d).

a form such that the update stage of the EKF utilizes this relative pose thereby providing reliable pose estimates for all the members of the team. The observation model and two approaches for cooperative localization are detailed in the following paragraphs.

4.1. *Observation Model for Heterogeneous Cooperative Localization*

Let us consider the case when the team is comprised of two robots. When robots #1 and #2 meet, they exchange relative pose information and the observation model becomes:

$$\mathbf{z}_{c_k} = \begin{bmatrix} x_{1_k} - x_{2_k} \\ y_{1_k} - y_{2_k} \\ \phi_{1_k} - \phi_{2_k} \end{bmatrix} + v_{12_k} = \mathbf{H}_{12_k}\mathbf{x}_{c_k} + v_{12_k} \qquad (3)$$

where $\mathbf{x}_{c_k}$ is a collective state vector resulting from exchanging relative pose information and v_{12_k} refers to the uncertainty present in the relative pose observation and is modeled as a zero-mean uncorrelated Gaussian sequence with covariance $\mathbf{R}_{12_k}$.

The residual and the residual covariance are:

$$\nu_{c_k} = \mathbf{z}_{c_k} - \hat{\mathbf{z}}_{c_k} = \mathbf{z}_{c_k} - \mathbf{H}_{12_k}\mathbf{x}_{c_{(k|k-1)}}$$
$$\mathbf{S}_{c_k} = \mathbf{H}_{12_k}\mathbf{P}_{c_{(k|k-1)}}\mathbf{H}_{12_k}^T + \mathbf{R}_{12_k}$$

The Kalman gain matrix, the state estimate and covariance updates (centralized) are as below:

$$\mathbf{W}_{c_k} = \mathbf{P}_{c_{(k|k-1)}}\mathbf{H}_{12_k}^T\mathbf{S}_{c_k}^{-1}$$
$$\mathbf{x}_{c_{(k|k)}} = \mathbf{x}_{c_{(k|k-1)}} + \mathbf{W}_{c_k}\left[\mathbf{z}_{c_k} - \left(\mathbf{x}_{1_{(k|k-1)}} - \mathbf{x}_{2_{(k|k-1)}}\right)\right]$$
$$\mathbf{P}_{c_{(k|k)}} = \mathbf{P}_{c_{(k|k-1)}} - \mathbf{W}_{c_k}\mathbf{S}_{c_k}\mathbf{W}_{c_k}^T$$

where $\mathbf{x}_{c_{(k|k-1)}}$ and $\mathbf{P}_{c_{(k|k-1)}}$ are the collective state and covariance predictions, respectively.

4.2. Laser-Based Cooperative Localization

Suppose that robot #2 has a scanning laser rangefinder and also that the number of satellites in view from the current position of this robot indicates that DGPS is unavailable. (In the field trial, this corresponded to the robot going under a tree.) Given the pose of robot #1 whose on-board sensors indicate a high level of confidence in their measurements, relative pose between robots #2 and #1 is determined as below:

- Robot #2 identifies robot #1 and acquires a range and bearing laser scan.
- Robot #1 communicates its pose to robot #2.
- After necessary preprocessing to discard readings that are greater than a predefined threshold, the range and bearing to the minima identified in the laser profile of robot #1 are determined as shown in Fig. 3.
- From the range and bearing pertaining to the minima, the pose of robot #2 is then inferred.
- Since robot #1 makes its pose available to robot #2, relative pose information is obtained by comparing the two poses and is now available for use in Eq. (3).

Within the EKF framework, state prediction takes place as before on individual robots according to Eq. (2) in a decentralized and distributed fashion. By exchanging relative pose information, the states of the robots are updated in a centralized fashion as detailed in Section 4.1.

The results for the laser-based cooperative localization are shown in Fig. 4. Figure 4(a) shows the estimated paths of robots #1 and #2. The pose standard deviations of robot#2 in Fig. 4(b) demonstrate the utility of the relative pose information in accomplishing cooperative localization. At *time* = 21 seconds, DGPS becomes unavailable as indicated by the rise in the x standard deviation. It can be seen that as a result of the laser-based relative position information, there is a sharp decrease in the position standard deviations of robot #2 (marked by arrows). As the motion of the robot is primarily in the x direction when the corrections are provided, the resulting decrease in the x standard deviation is noticeable compared to those in y and ϕ.

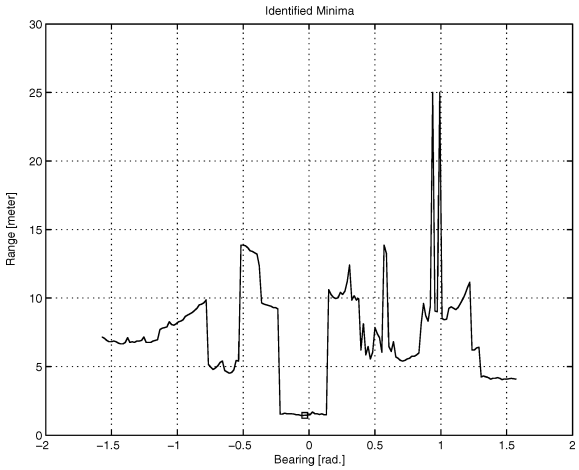

Figure 3. Laser-based cooperative localization. The square (□) denotes the identified minima from laser rangefinder scans.

4.3. Vision-Based Cooperative Localization

In this approach, the PTZ camera that is part of the sensor suite is used to provide relative position information. Consider the case where two robots are performing cooperative localization with the camera-equipped robot #1 lacking in absolute positioning capability. Relative position information is obtained as follows: First, robot #1 searches the vicinity for another robot (say, robot #2) whose pose is known (this is determined via TCP/IP message passing). Robot #1 then visually acquires robot #2 using an object recognition algorithm. The algorithm identifies the centroid of the robot within the image frame using a color segmentation scheme and marks its pixel coordinates on that frame. Figure 5(a)–(d) show the marked coordinates for various robot positions.

An incremental depth-from-motion algorithm (look ahead to Section 5.2 for further details) computes the

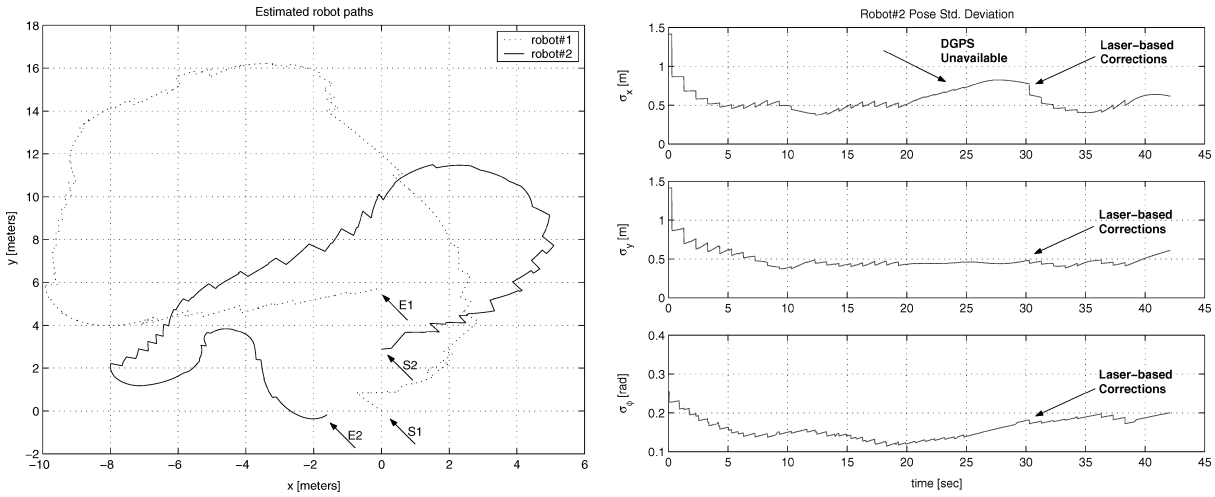

Figure 4. The robots perform laser-based cooperative localization when DGPS becomes unavailable or when there are not enough satellites in view. EKF estimated robot paths are shown in (a). The solid line denotes the estimated path of robot #2 and the dotted line that of robot #1. (S1,E1) and (S2,E2) denote the start and end positions for robots #1 and #2, respectively. The standard deviations of the pose of robot #2 during laser-based cooperative localization are shown in (b). The external corrections offered by the laser-based localization scheme are marked by arrows.

Figure 5. Vision-based cooperative localization. The circles (○) denote the pixel coordinates (see text for details).

range for a window within the frame which encloses these coordinates.

The required relative position is inferred from the computed range and the bearing of robot #2 relative to robot #1 is approximately determined from the lateral displacement between the enclosed pixel coordinates and the coordinates of the frame's optical center. Owing to the 160×120 pixel frame size in the present case and the 37° FOV, 1 pixel of lateral displacement from the optical center corresponds to 0.225° relative bearing, provided nonlinear effects due to lense distortion are ignored. The robot states are then updated as detailed in Section 4.1.

The terrain mapping is then performed using the robot pose provided by the EKF. The next section details the same.

5. Terrain Mapping

Incremental terrain mapping takes place via four main processes. Firstly, an incremental dense depth-from-camera-motion algorithm is used to compute ranges to various features in the environment. The relative pose and associated range covariances are used to specify regions with OOIs. Then, an elevation gradient is determined by fusing DGPS altitude information with vertical displacements obtained from the inclinometer pitch angles as the robot moves. The range and elevation information are then registered with their associated covariances. Finally, the map is updated to incorporate the registered values at their proper coordinates. Covariances associated with these measurements provide a confidence measure of range determination. When

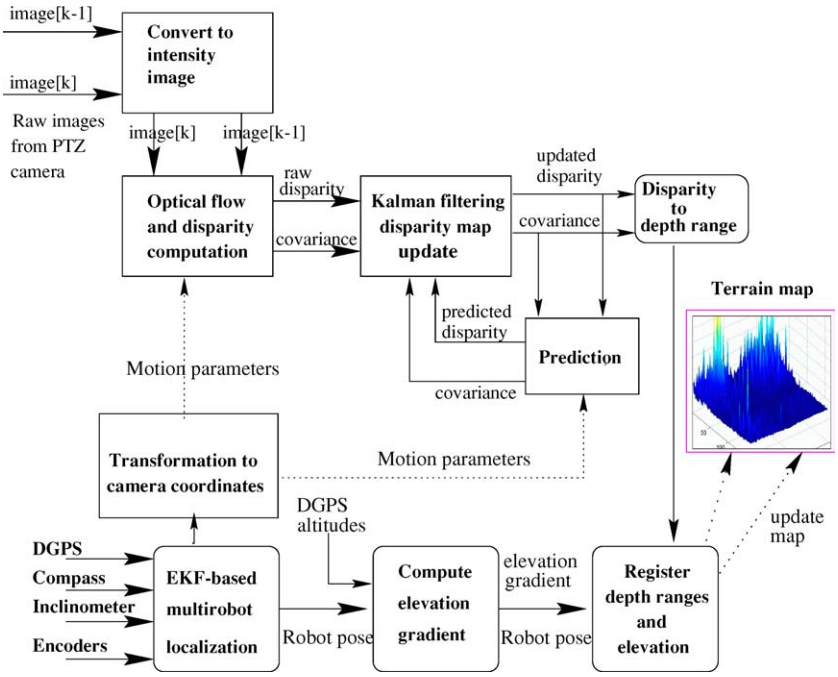

Figure 6. The overall terrain mapping scheme.

more than one robots explore the same area, this confidence determines whether or not the map gets updated.

The overall schematic diagram of the algorithm is shown in Fig. 6. Details about the implementation of each block are discussed next.

5.1. Terrain Traversal Procedure

Each member of the robot team traverses the environment systematically using the logic depicted in Fig 7.

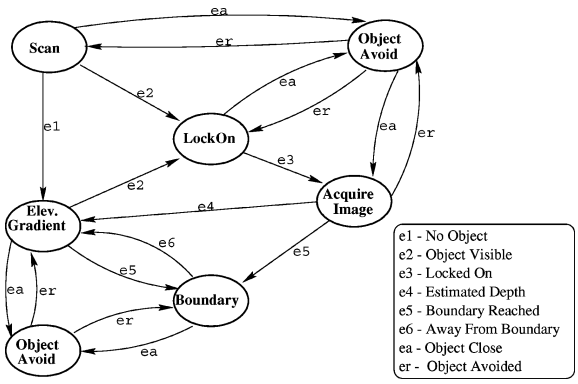

Figure 7. Terrain traversal logic.

In the `scan` mode, the robot turns in place while scanning the environment noting objects of interest, their relative orientation and a confidence measure of which objects are more clearly observed than others. The most visible object is selected (`LockOn`) and its range is estimated (`AcquireImage`). The robot then moves towards this object while computing changes in the elevation across the terrain (`ElevGradient`). The robot turns away from the object (`ObjectAvoid`) when it gets too close but notes the object's location in the global frame so that it can be indicated on the global terrain map. A different object is selected and the procedure is repeated. The robot also backs away from regions where it may tilt over (`Boundary`). `Boundary` and `ObjectAvoid` are fail-safe modes to enhance the robot's survivability. An agent-based coordinated control scheme designed for this traversal procedure is described in Fregene (2002).

5.2. Range Determination

The range of environmental features are determined from the optical flow between frames during small (known) camera motion. Assume a right handed

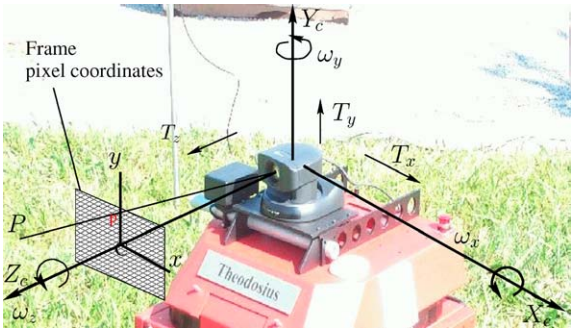

Figure 8. Camera model and coordinates.

coordinate system for the camera as shown in Fig. 8. Two simple homogeneous transformations are required to go from the robot coordinate frame to the camera coordinates. This transformation from **c**amera to **r**obot can be represented as

$$H_c^r : [X_c\ Y_c\ Z_c\ 1]^T \rightarrow [X\ Y\ Z\ 1]^T$$

where

$$H_c^r = \begin{bmatrix} R_{z,\frac{\pi}{2}} R_{x,\frac{\pi}{2}} & \mathbf{0} \\ \mathbf{0} & r \end{bmatrix}$$

and r is the position vector of the camera center relative to the robot center of gravity while R_x, R_z are rotation matrices about the indicated axes.

In the camera frame, each point in a scene has an associated position vector $P = (X_c, Y_c, Z_c)^T$. This is projected onto $p = (x, y)^T$ in the image plane using the perspective projection:

$$x = \frac{fX_c}{Z_c}, \quad y = \frac{fY_c}{Z_c}$$

where f is the focal length of the projection and the point is located at a *depth* Z_c from the camera center. The image coordinate system is assumed centered at a center of projection corresponding to the frame center. On this basis, a simple camera model (see Sobel, 1974) is used to obtain the transformation from (x, y) in the image plane to actual pixel row and column. Define $T = (T_x, T_y, T_z)^T$ and $\Omega = (\omega_x, \omega_y, \omega_z)^T$ as the translational and rotational velocities of the point due to camera motion. Then the image velocity $V(x, y)$ is given by:

$$V(x, y) = d(x, y)\mathbf{F}(x, y)T + \mathbf{G}(x, y)\Omega \qquad (4)$$

where $d(x, y) = \frac{1}{Z_c}$ is the inverse depth (or *disparity*) and

$$\mathbf{F}(x, y) = \begin{bmatrix} -f & 0 & x \\ 0 & -f & y \end{bmatrix},$$

$$\mathbf{G}(x, y) = \begin{bmatrix} \frac{xy}{f} & -\frac{f+x^2}{f} & y \\ \frac{f+y^2}{f} & -\frac{xy}{f} & -x \end{bmatrix}$$

The motion parameters T and Ω in Eq. (4) can be either estimated from the EKF-based localization algorithm or numerically computed from sensor data and post-processed. Accordingly, the only unknowns are the inverse depth $d(x, y)$ and the image velocity $V(x, y)$. For small motions between frames, $V(x, y)$ corresponds to the *optical flow* (Matthies and Kanade, 1989). Thus, computing the optical flow for each pixel in the image frame provides a way to estimate dense depth from camera motion and thus the range of environmental features.

The optical flow between two successive frames (and associated variances) are obtained by a sum of squared difference (SSD) correlation-based algorithm (Fregene et al., 2002). This algorithm runs until the entire frame has been processed. The variance associated with the optical flow is determined by fitting the flow corresponding to the smallest SSD and its two nearest neighbors to a parabola. Raw disparity is computed from Eq. (4) and fused with predicted disparity using a Kalman Filter (see Fregene et al. (2002) and Matthies and Kanade (1989) for a detailed discussion). The next frame is then processed in the same way and so on till the variance indicates that the range has been estimated with sufficiently high accuracy.

5.3. *Obtaining an Elevation Gradient*

Initially, a coordinate frame is fixed local to the area of interest (but global from the viewpoint of the members of the robot team). Pose measurements are therefore referenced to the same coordinate system. The 3D pose of the robot at the start location is noted, then the vision-based range determination algorithm is run. The robot advances to a location near the most visible object. GPS readings are used to determine vertical displacement of the robot between these two locations. This is fused with another vertical displacement measure based on the inclinometer pitch angle θ as follows:

Let L be the offset between the robot's center of gravity and the camera's optical center, *NOS* the number

of satellites acquired, Z_g the altitude reading from the DGPS and Z_{g0} the DGPS-measured altitude at the base station location. Then, the elevation gradient ΔZ is obtained as:

$$\Delta Z = \frac{1}{2}[\underbrace{f_\theta L \tan\theta}_{\text{inclinometer}} + \underbrace{f_{\text{gps}}(Z_g - Z_{g0})}_{\text{DGPS}}],$$

where

$$f_{gps} = \begin{cases} 0.1 & NOS \leq 4 \\ \dfrac{NOS}{10} & 4 < NOS \leq 10 \\ 0.9 & NOS > 10 \end{cases}$$

$$f_\theta = \begin{cases} 0.9 & NOS \leq 4 \\ \left(1 - \dfrac{NOS}{10}\right) & 4 < NOS \leq 10 \\ 0.1 & NOS > 10 \end{cases}$$

We assume at the start that $Z_g = Z_{g0}$ and $\theta \approx 0$ so that the nominal starting value for ΔZ is zero. That is, the terrain is assumed flat until robots actually traverse specific portions and update the elevation information. In this formulation, the number of satellites acquired by the GPS is used as a measure of the confidence associated with the vertical displacements provided by the GPS. The vertical displacements are monitored between two positions, say P_1 and P_2 as in Fig. 9 to give an elevation profile for that motion segment corresponding to the depth map obtained. These range and elevation information are registered to a local map which essentially encapsulates the terrain information within the robot's FOV between the two locations. At P_2, the robot turns away from objects, their locations are marked, then new range information is obtained. The robot advances to a point P_3, then creates a local map connecting P_2 and P_3 containing range and elevation information. This process continues with each robot updating the global map as information significantly different from what is already registered on that map becomes available. The map making is incremental in the sense that the terrain is effectively partitioned into segments corresponding to the location of OOIs.

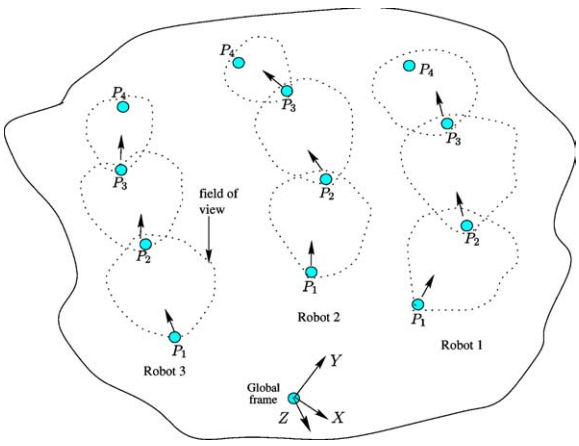

Figure 9. Obtaining an elevation gradient.

5.4. *Elevation-Range Registration*

The terrain is represented by a terrain matrix $\mathcal{T}$ whose rows/columns indices (i, j) correspond to X, Y coordinates (in the global frame) and the associated values at these indices contain the elevation gradient at that point. Then the terrain matrix elements are given by:

$$\mathcal{T}_{ij} = \begin{cases} \Delta Z|_{XY} & \text{explored region} \\ \mathbf{0} & \text{unexplored region} \end{cases} \quad (5)$$

Range data from multiple viewpoints correspond to different row/column indices on $\mathcal{T}$. Accordingly, registration simply consists of matching the position coordinates (X, Y) within the immediate FOV of the robot with vertical displacements and updating the matrix $\mathcal{T}$ according to Eq. (5). This registration is done after each robot traverses the region between two points, (say, P_1 and P_2 in Fig. 9). When necessary, gaps are filled in by cubic interpolation so that when the robot arrives at P_2, a 3D map of a subset of the region it just departed is created. It is straightforward to mark object locations by assigning matrix entries with much larger magnitudes than surrounding locations. Bearing information is calculated from the camera's angle of view and the number of pixels per frame.

This process is made simpler because (a) there is a global coordinate frame in which all measurements are expressed; (b) all the information to be fused are available in metric (rather than topological) form; and (c) the manner in which exploration is carried out implicitly takes depth information into account.

5.5. *Updating the Terrain Map*

The local maps generated by each of the mapping robots are combined into a global map based on the

XYZ coordinate frame. For previously unmapped regions, the global map is updated as soon as the registration step is completed. The variances associated with the range determination and the number of sensed GPS satellites may be utilized as confidence measures when the same region is traversed more than once. The global map update then depends on these confidence measures. However, the experimental results we report are based only on a *one-pass* update. The resulting map is itself a metric map represented by the terrain matrix from which a 3D surface is subsequently generated.

6. Experimental Results for Mapping

Our experiments show results obtained using two robots (`Augustus` and `Theodosius`) in an outdoor environment. The robots move slowly around the environment such that the average inter-frame displacement is no more than 2 centimeters.

The scenery within the robot `Augustus`' FOV during this particular motion segment is shown in Fig. 10(a). The prominent object in this scenery is a tree behind which is a building. The filtered depth map recovered for every pixel is shown in Fig. 10(b). In this case, the lighter the area, the closer it is to the robot. Thus, using the mapping scheme described in Fig. 9, the next motion segment for this robot starts on the other side of the tree that is located about 10 meters from the robot. Its orientation relative to the robot is obtained from the lateral pixel displacement relative to the center of the image frame. It should be noted that the sky line and the borders of the building behind the tree are too far away for their depth estimates to be reliable. Covariance plots which indicate how reliable the inferred depth of each pixel is can be found in Fregene et al. (2002). They are not included here due to space constraints. Figure 10(c) shows the scenery within the FOV of `Theodosius`. The prominent features here are several culvert covers with a tree branch just overhanging them. The recovered depth map is depicted in Fig. 10(d).

The paths which correspond to the motion segment at this instant are shown in Fig. 11. The solid lines

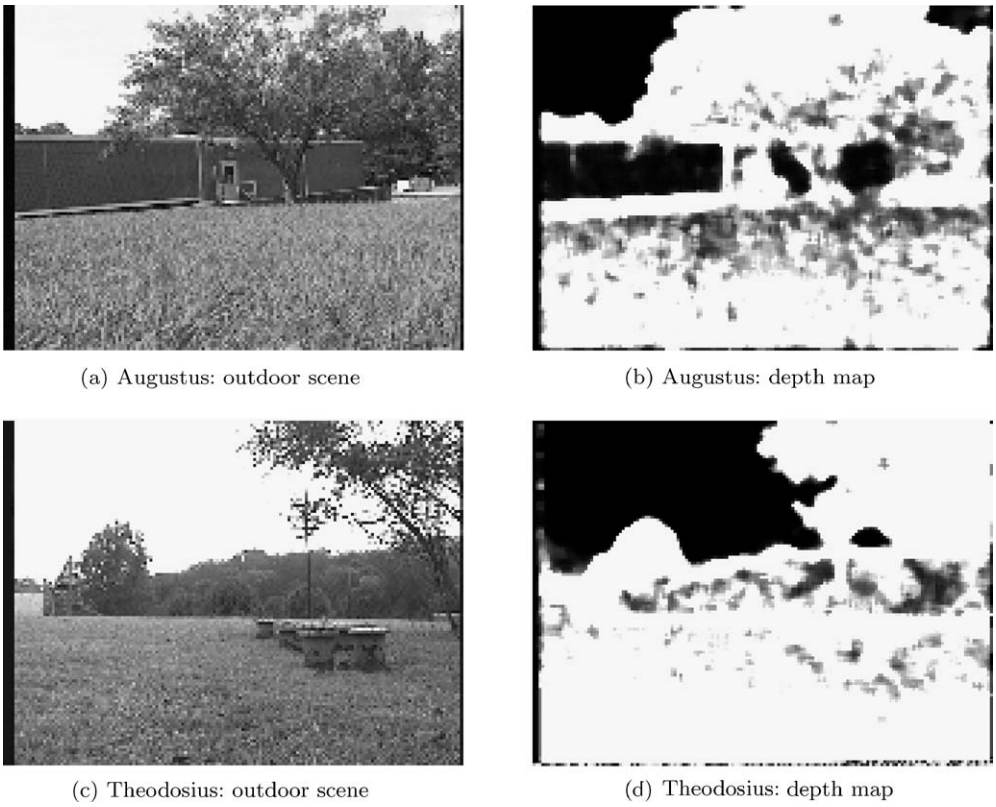

(a) Augustus: outdoor scene

(b) Augustus: depth map

(c) Theodosius: outdoor scene

(d) Theodosius: depth map

Figure 10. Experimental results for `Augustus` and `Theodosius`.

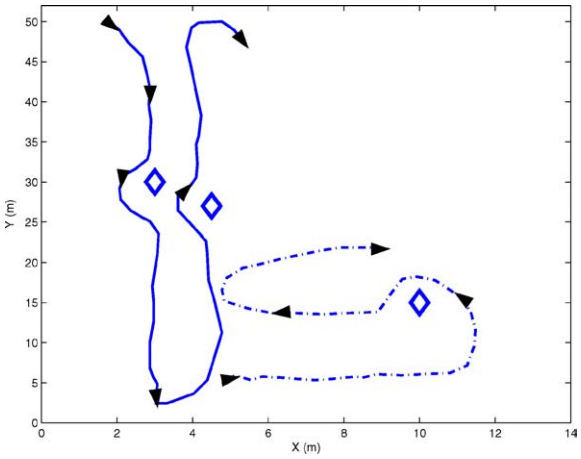

Figure 11. Robots' path during a particular mapping segment.

correspond to the path of the robot `Theodosius` while the dash-dot lines show the path of the robot `Augustus` during this segment. The fact that the path data is not smooth is because the GPS position update used in localization is much slower than position encoders internal to the vehicles (see the third column of Table 1 for relevant frequency values). The diamonds in Fig. 11 represent the location of the objects in the terrain.

Both the elevation profile for the motion segments and the feature locations are mapped as shown in the partially updated terrain map (Fig. 12). It shows the elevation profile across the area traversed by each robot (in the locally fixed coordinate frame centered at the LADGPS base station location) and prominent features within the robot's FOV during the motion segment are marked on the map. This terrain map is essentially a visualization of the terrain matrix $\mathcal{T}$. Areas with prominent features have $\mathcal{T}_{ij}$ entries several orders of magnitude higher than the neighboring displacement entries which serves to flag them as areas to be avoided. Portions of the terrain still unexplored by the robots contain no elevation information at the instant shown. Once markers are placed at the approximate locations of the environmental features, exploration then continues on the other side of these markers (this is illustrated in the area explored by the robot `Theodosius` in Fig. 12). A map of the entire terrain under consideration is not shown since it would essentially provide similar information (i.e., X, Y coordinates with associated elevation gradient) to the results shown for the explored area.

Although the scenery within both robots' FOV as shown in Fig. 10(a) and (c) appear to be relatively flat (due to the tall grass growing on the terrain), this is not really the case. The terrain is actually fairly undulatory. To show this, the scale of the vertical displacement measure (ΔZ) is slightly exaggerated in Fig. 12.

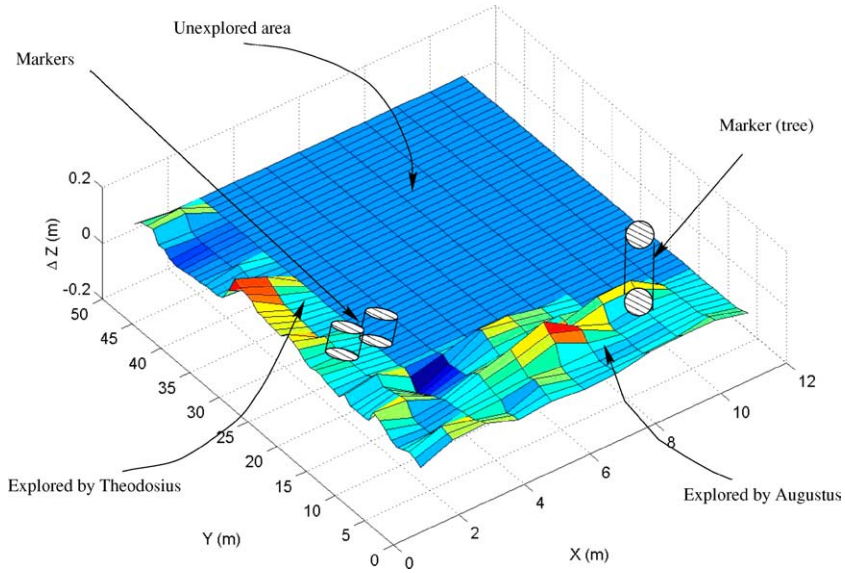

Figure 12. Partially updated terrain map.

7. Conclusions and Further Research

This article presented a scheme for localization and terrain mapping for a team of robots operating in uneven and unstructured environments. To localize the robots within the environment, a distributed multirobot EKF-based algorithm was described. For cases where all robots of the team may not have absolute positioning capabilities, it was shown how cooperative localization can be performed exploiting heterogeneous sensors aboard the team members. The multirobot terrain mapping algorithm used localization information to combine vision-based range estimates with an elevation profile across the terrain. This profile was obtained by fusing vertical displacements from the DGPS with those computed from inclinometer pitch angles while the robots traverse the terrain of interest. The proposed scheme was successfully implemented using real data obtained from field trials with no modification to the operating environment or to the robots of the team. Experimental results demonstrated the application of this scheme to a terrain mapping problem that is partly motivated by path planning requirements.

There are several ways to extend this work. For instance, other robots equipped with laser rangefinders can be included in the mapping scheme to improve the bearing accuracy of features located in the environment. In this case, range estimation can be done with greater accuracy by comparing vision-based and laser-based ranges. From a computational standpoint, it is probably sufficient to employ a feature-based (rather than iconic) depth estimation scheme since it is not usually necessary to mark the ranges to the entire FOV on the elevation profile. For this to be useful, the algorithm should track OOIs rather than every pixel in the frame. Although the map update shown in the experiments would typically suffice for path planning in static or slowly changing environments, this may not be the case for dynamic environments. Therefore schemes to update the maps online in dynamic environments would be a significant extension to this work.

An entropy-based information metric developed in Madhavan (2001) can be used to evaluate the *information content* of an observation before that observation is used for cooperative localization thereby enabling the incorporation of observations that provide the maximum information towards localization. It is easy to utilize this metric within the proposed estimation-theoretic framework. Extended Information filtering (EIF) (Maybeck, 1979), a variant of EKF, has been widely touted in recent years as an antidote for the problems associated with EKF schemes. For the current application, the large matrix inversions necessitated by the EIF make it unsuitable. *Global Localization* is the ability to estimate the position of a robot without knowledge of its initial location and the ability to *relocalize* if its position is lost (referred to as the "kidnapped robot problem" in the literature). Recently, Howard et al. (2003) have developed a Bayesian indoor cooperative localization framework that is able to self-initialize and self-correct using laser and camera to detect coded-fiducials placed on the robots and as such requires modifications to the robots of the team. Global cooperative localization that does not compromise the advantages of our distributed heterogeneous framework will be a nice addition to this work and will result in a robust outdoor cooperative localization and mapping (CLAM) scheme. Furthermore, as the number of robots in the team increases, it may no longer be sufficient (or indeed practical) to merely use the pose of one robot to estimate the pose of another (as described in Section 4) since this could conceivably lead to conditional dependencies of the pose estimates. Accordingly, a useful extension of this work would be efficient cooperative localization that exploits heterogeneity with reduced (or no) conditional dependence. All these issues remain the subject of further research effort.

Acknowledgments

The research reported in this article has been authored by contractors of the U.S. Government under Contract No. DE-AC05-00OR22725 with UT-Battelle, LLC. The U.S. Government retains a nonexclusive royalty-free license to publish or reproduce the published form of this contribution, or allow others to do so, for U.S. Government purposes. Research sponsored by the Engineering Research Program of the Office of Basic Energy Sciences, U.S. Department of Energy. Commercial equipment and materials are identified in this article in order to adequately specify certain procedures. Such identification does not imply recommendation or endorsement by the National Institute of Standards and Technology, nor does it imply that the materials or equipment identified are necessarily the best available for the purpose.

Note

1. *A group of robots is defined to be homogeneous if the capabilities of the individual robots are identical and heterogeneous otherwise* (Cao, 1997). Homogeneous robots may be considered to have exactly identical hardware and software abilities. Heterogeneity is manifested either as physical or behavioral differences.

References

Bison, P. and Trainito, G. 1996. A robot duo for cooperative autonomous navigation. In *Proc. of Dist. Auton. Rob. Syst. 2*, pp. 423–430.

Burgard, W., Moors, M., Fox, D., Simmons, R., and Thrun, S. 2000. Collaborative multi-robot exploration. In *Proc. of the IEEE Intl. Conf. on Rob. & Autom.*, vol. 1, pp. 476–481.

Cao, Y., Fukunaga, A., and Kahng, A. 1997. Cooperative mobile robotics: Antecedents and directions. *Auton. Robots*, 4(1):7–27.

Di Marco, M., Garulli, A., Giannitrapani, A., and Vicino, A. 2003. Simultaneous localisation and map building for a team of cooperating robots: A set membership approach. *IEEE Trans. on Rob. & Autom.*, 19:238–249.

Dudek, G., Jenkin, M., Milios, E., and Wilkes, D. 1993. Robust positioning with a multi-agent robotic system. In *Proc. of the Intl. Joint Conf. on Artificial Intelligence Workshop on Dynamically Interacting Robots*.

Economou, J.T. 1999. *Modelling and Control of Skid Steer Vehicles*. Ph.D. thesis, Royal Military College of Science, Cranfield University.

Feddama, J., Lewis, C., and Lafarge, R. 2000. Cooperative sentry vehicles and differential GPS leapfrog. In *Proc. of Dist. Auton. Rob. Syst.*, pp. 293–302.

Fox, D., Burgard, W., Kruppa, H., and Thrun, S. 1999. Collaborative multi-robot localization. In *Proc. of the 23rd Annual German Conf. on Artificial Intelligence*, pp. 255–266.

Fregene, K. 2002. *Distributed Intelligent Control of Hybrid Multiagent Sytems*. Ph.D. thesis, Department of Electrical and Computer Engineering, University of Waterloo, Ontario, Canada.

Fregene, K., Madhavan, R., and Parker, L.E. 2002. Incremental multiagent robotic mapping of outdoor terrains. In *Proc. of the IEEE Intl. Conf. on Rob. & Autom.*, May, pp. 1339–1346.

Gage, D.W. and Pletta, J. 1987. Ground vehicle convoying. In *Proc. of the SPIE Conf. on Mobile Robots II*, vol. 852, pp. 319–327.

Grabowski, R., Navarro-Serment, L.E., Paredis, C.J., and Khosla, P.K. 2000. Heterogeneous teams of modular robots for mapping and exploration. *Auton. Robots*, 8(3):271–298.

Howard, A. and Kitchen, L. 1999. Cooperative localisation and mapping: preliminary report. Technical Report TR1999/24, Dept. of Computer Science & Software Engineering, The University of Melbourne.

Howard, A., Matarić, M., and Sukhatme, G. 2003. Putting the 'I' in 'Team': An ego-centric approach to cooperative localization. In *Proc. of the IEEE Intl. Conf. on Rob. & Autom.*, Sept., pp. 868–892.

Jennings, C., Murray, D., and Little, J. 1999. Cooperative robot localization with vision-based mapping. In *Proc. of the IEEE Intl. Conf. on Rob. & Autom.*, vol. 4, pp. 2659–2565.

Jung, I-K., Lacroix, S., Mallet, A., Chatila, R., and Devy, M. 2002. Simultaneous localisation and digital elevation map building from aerial stereo imagery. In *Intl. Conf. on Rob. & Autom. Workshop on "Concurrent Mapping and Localization for Auton. Mobile Robots"*.

Kurazume, R., Hirose, S., Nagata, S., and Sashida, N. 1996. Study on cooperative positioning system (basic principle and measurement experiment). In *Proc. of the IEEE Intl. Conf. on Rob. & Autom.*, vol. 2, pp. 1421–1426.

Little, J., Jennings, C., and Murray, D. 1998. Vision-based mapping with cooperative robots. In *Proc. of SPIE—Sensor Fusion and Decentralized Control in Rob. Syst.*, vol. 3523, May, pp. 2–12.

Madhavan, R. 2001. *Terrain Aided Localisation of Autonomous Vehicles in Unstructured Environments*. Ph.D. thesis, School of Aeronautical, Mechanical and Mechatronic Engineering, The University of Sydney, Sydney, Australia.

Madhavan, R., Fregene, K., and Parker, L.E. 2002. Distributed heterogeneous outdoor multi-robot localization. In *Proc. of the IEEE Intl. Conf. on Rob. & Autom.*, May, pp. 374–381.

Matthies, L. and Kanade, T. 1989. Kalman filter-based algorithms for estimating depth from image sequences. *Intl. Jrnl. of Comp. Vision*, 3:209–236.

Maybeck, P. 1979. *Stochastic Models, Estimation, and Control*, vol. 1. Academic Press, New York.

Parker, L.E. 2000. Current state of the art in distributed robot systems. In *Dist. Auton. Syst.*, L.E. Parker, G. Bekey and J. Barhen (Eds.), vol. 4, pp. 3–12. Springer-Verlag.

Premvuti, S. and Wang, J. 1996. Relative position localizing system for multiple autonomous robots in distributed robotic system: System design and simulation. *Rob.s and Auton. Syst.*, 18:319–326.

Rekleitis, I.M., Dudek, G., and Milios, E.E. 1998. On multi-agent exploration. In *Proc. of Vision Interface*, pp. 455–461.

Roumeliotis, S. and Bekey, G. 2002. Distributed multi-robot localization. *IEEE Trans. on Rob. & Autom.*, 18(5):781–795.

Sanderson, A.C. 1996. Cooperative navigation among multiple mobile robots. In *Dist. Auton. Syst. 2*, H. Asama, T. Fukuda, T. Arai, and I. Endo (Eds.), pp. 389–400. Springer-Verlag.

Sobel, I. 1974. On calibrating computer-controlled cameras for perceiving 3-D scenes. *Artificial Intelligence*, 5:185–198.

Yamauchi, B. 1998. Frontier-based exploration using multiple robots. In *Proc. of the Second Intl. Conf. on Auton. Agents*, pp. 47–53.

Raj Madhavan received the Bachelor of Engineering degree (Electrical and Electronics) in 1995 from the College of Engineering, Anna University, India and the Master of Engineering (Research) degree (Control and Robotics) in 1997 from the Department of Engineering, The Australian National University, Australia. He received his Ph.D. degree (Field Robotics) in 2001 from the School of Aerospace, Mechanical and Mechatronic Engineering (Department of Mechanical and Mechatronic Engineering at the time of completion), The University of Sydney, Sydney, Australia.

Since 2001, he has been a research associate with the Oak Ridge National Laboratory (ORNL) and is currently a guest researcher with the Intelligent Systems Division of the National Institute of Standards and Technology (NIST). His current research interests include autonomous vehicle navigation in complex unstructured environments, performance metrics for intelligent systems, distributed heterogeneous sensing and systems and control theory. Dr. Madhavan is listed in Strathmore Who's Who, 2003–2004, America's Registry of Outstanding Professionals as an Honored Member 2003–2004, and United Who's Who, 2003–2005. He is also an elected full member of the scientific research society, Sigma Xi and the Washington Academy of Sciences and a member of IEEE, ASME and AIME. He was the Postgraduate winner of the 1998 IEEE Region 10 (Asia and the Pacific) Student Paper Competition and the Graduate Division winner of the 1998 Society for Mining, Metallurgy and Exploration (SME) Outstanding Student Paper Contest.

Kingsley Fregene received the B.Eng. degree (with first class honors) in electrical and computer engineering from the Federal University of Technology, Owerri, Nigeria, in 1996, and the M.A.Sc. and Ph.D. degrees in electrical and computer engineering from the University of Waterloo, ON, Canada, in 1999 and 2002, respectively. He held Summer research positions at the Los Alamos National Laboratory, Los Alamos, NM in 1999 and at Oak Ridge National Laboratory, Oak Ridge, TN, in 2001.

Dr. Fregene is currently a Research Scientist with Honeywell Laboratories, Minneapolis, MN in the Aerospace Electronic Systems Center of Excellence. His current research interests are in intelligent systems, applied nonlinear control, guidance, navigation and coordinated control of autonomous air/ground vehicle teams. He is a member of the IEEE and AIAA.

Lynne E. Parker received the Ph.D. degree in computer science in 1994 from the Massachusetts Institute of Technology (MIT), Cambridge, performing research on cooperative control algorithms for multirobot systems in MITís Artificial Intelligence Laboratory. She joined the faculty of the Department of Computer Science at the University of Tennessee, Knoxville, as Associate Professor in August 2002, where she founded the Distributed Intelligence Laboratory. She also holds an appointment as Adjunct Distinguished Research and Development Staff Member in the Computer Science and Mathematics Division at Oak Ridge National Laboratory, Oak Ridge, TN, where she worked as a Researcher for several years. She is the author of three edited volumes on the topic of multirobot systems. Her current research interests are in distributed robotics and artificial intelligence.

Dr. Parker was awarded the 2000 Presidential Early Career Award for Scientists and Engineers for her research in multirobot systems. She serves on numerous international conference program committees and was the primary conference organizer and program committee chair for the IEEE sponsored Fifth International Symposium on Distributed Autonomous Robotic Systems (DARS 2000) in October, 2000. She co-organized the Second International Workshop on Multirobot Systems held at the Naval Research Laboratory in March, 2003.